DOI 10.7343/as-2026-946

ACQUE SOTTERRANEE
Italian Journal of Groundwater
journal homepage: https://www.acquesotterranee.net/

flowpath TORINO 2025
11th-13th June | National Meeting on Hydrogeology

# Hydrogeological monitoring of groundwater resources within the High Valley of theTenna River (Sibillini Mts. Range, Central Italy) and possible near-field effects from the 2016-2017 Central Italy seismic sequence

## *Monitoraggio idrogeologico delle risorse idriche sotterranee dell' Alta Valle del Fiume Tenna (Monti Sibillini, Italia centrale) e possibili effetti di prossimità indotti dalla sequenza sismica dell'Italia centrale del 2016-2017*

**Lucio Martarelli[a] , Rossella Maria Gafà[a], Francesco La Vigna[a], Gennaro Maria Monti[a], Angelantonio Silvi[a], Angelo Cipriani[a]**

a - Servizio Geologico d'Italia - ISPRA - Via V. Brancati, 48 - 00154 - Roma, Italia

email: *lucio.martarelli@isprambiente.it; rossella.gafa@isprambiente.it; francesco.lavigna@isprambiente.it; gennaro.monti@isprambiente.it; angelo.silvi@isprambiente.it; angelo.cipriani@isprambiente.it*

**ARTICLE INFO**

Ricevuto/*Received*: 7 January 2026
Accettato/*Accepted*: 16 June 2026
Pubblicato online/*Published online*: 30 June 2026

**Handling Editor**:
**Stefania Da Pelo**

**Editor in Chief:**
**Stefania Da Pelo**

**Citation:**
Martarelli, L., Gafà, RM., La Vigna, F., Monti, GM., Silvi, A., Cipriani, A., (2026). Hydrogeological monitoring of groundwater resources within the High Valley of the Tenna River (Sibillini Mts. Range, Central Italy) and possible near-field effects from the 2016-2017 Central Italy seismic sequence
Acque Sotterranee - *Italian Journal of Groundwater*, 15(2), 23 - 38
https://doi.org/10.7343/as-2026-946

**Correspondence to:**
**Lucio Martarelli**
*lucio.martarelli@isprambiente.it*

**Keywords:** *hydrogeology, groundwater resources, coseismic effects, Sibillini Mts., Central Italy.*

**Parole chiave:** idrogeologia, risorse idriche sotterranee, effetti cosismici, Monti Sibillini, Italia centrale.



### Abstract

*The high valley of the Tenna River is in the central-eastern part of the Sibillini Mts., Central Italy. Within a research agreement between the Sibillini Mts. National Park and the Geological Survey of Italy of ISPRA, hydrogeological surveys aimed to characterize the study area and evaluate possible near-field effects of the 2016-2017 Central Italy seismic sequence on the local groundwater resources started in June 2018 and were performed until July 2020. Stream discharge and hydrochemical in situ measurements were carried out.*

*The hydrogeological conceptual model built through a rectified cross section along the high valley of the Tenna River suggested that Capotenna sector acts as a groundwater recharge area. In this area, a possible post-seismic groundwater depletion, although not adequately quantified because of limited availability of continuous pre-seismic monitoring data, may have enhanced the depletion already induced by recent snow-rainfall "decrease". During the monitoring period, the Scaglia Aquifer at Capotenna had seldom sufficient hydraulic potential to allow the drainage through the underlying marly low permeability threshold. Along Tenna streambed, at 1175-990 m a.s.l., groundwater inputs from the Basal Calcareous Aquifer and Maiolica Aquifer were evidenced, this latter by overflow on a low permeability formation. At lower elevation (985-845 m a.s.l.), in a sector featured by the Basal Calcareous Aquifer, a complex situation of hydraulic exchange between groundwater and surface water was found, likely due to tectonic fragmentation of hosting rocks and/or to the quite thin aquifer sustained by low permeability layers (evaporitic and marly deposits).*

*The main contributions of this paper, with respect to previous studies on the hydrogeological effects of the 2016-2017 seismic sequence in Sibillini Mts., were the reconstruction of a local conceptual model, the analysis of groundwater-surface water exchanges along the Tenna River, and the identification of elevation sectors with different hydraulic behavior.*

### Riassunto

L'alta valle del Fiume Tenna è ubicata nella parte centro-orientale dei Monti Sibillini (Italia centrale). Nell'ambito di una collaborazione di ricerca tra Ente Parco Nazionale dei Monti Sibillini ed il Servizio Geologico d'Italia di ISPRA sono stati svolti rilievi idrogeologici finalizzati alla caratterizzazione dell'area di studio ed alla valutazione dei possibili effetti cosismici di prossimità della sequenza sismica 2016-2017 nell'Italia centrale. Le attività, iniziate nel giugno 2018, sono state condotte fino a luglio 2020. Sono state eseguite misure di portata in alveo e di parametri idrochimici in situ. Il modello concettuale idrogeologico ricostruito in una sezione rettificata lungo l'alto corso del Fiume Tenna ha suggerito che il settore di Capotenna ha un ruolo di area di ricarica delle acque sotterranee. In questo settore, una possibile diminuzione di disponibilità di risorse idriche sotterranee nel primo periodo post-sismico, sebbene non adeguatamente quantificata a causa della limitata disponibilità di dati di monitoraggio in continuo nel periodo pre-sismico, si è sommata a quella già indotta dalla recente minore disponibilità di precipitazioni nivo-pluviometriche. Durante il periodo del monitoraggio di questo studio, l'Acquifero della Scaglia Calcarea a Capotenna ha raramente avuto un sufficiente potenziale idraulico per consentire il drenaggio attraverso la locale soglia a bassa permeabilità. Al contrario, le risorse idriche sotterranee situate a minore quota lungo il corso del Fiume Tenna hanno avuto un limitato e breve periodo di incremento post-sismico, presto ristabilito alla situazione pre-sisma dopo l'estate 2020. Lungo l'alveo del Tenna, tra le quote 1175 e 990 m s.l.m., sono stati evidenziati trasferimenti idrici verso le acque superficiali dall'Acquifero Calcareo Basale e dall'Acquifero della Maiolica, da quest'ultimo per travaso sulla soglia di una formazione marnosa. A quote ancora più basse (985-845 m s.l.m.), in un settore caratterizzato dalla presenza dell'Acquifero Calcareo Basale, è stata rilevata una complessa situazione di scambio idraulico tra acque sotterranee e superficiali, probabilmente dovuta alla frammentazione delle rocce serbatoio e/o alla relativamente poca potenza dell'acquifero qui sostenuto da alcuni strati a bassa permeabilità (depositi evaporitici e marnosi). I principali contributi del presente lavoro, rispetto agli studi precedenti sugli effetti idrogeologici della sequenza sismica 2016-2017 nei Monti Sibillini, sono stati la ricostruzione di un modello concettuale locale, l'analisi degli scambi idrici tra acque sotterranee e superficiali lungo il Fiume Tenna e l'identificazione del diverso comportamento idraulico di settori fluviali a differenti quote.

## Introduction

The present study has been conducted with the aim of defining a conceptual hydrogeological model which may contribute to the characterization and possible sustainable management of the available high valley of the Tenna River groundwater resource. The present study was developed according to the quantitative hydrogeology criteria (e.g., Mastrorillo et al., 2009; Boni et al., 1986; Boni and Bono, 1982), which are based on information and data collected by field hydrogeological surveys. Furthermore, it is noteworthy that the high valley of the Tenna River is located northward and close to the epicentral areas of the 2016-2017 seismic sequence.

The study of the coseismic effects on groundwater resources is a widely investigated topic at both Italian and international scale (e.g., Liu et al., 2023; Weaver et al., 2019; Mohr et al., 2016; Yan et al., 2014; Adinolfi Falcone et al., 2012; Cox et al., 2012; Wang and Manga, 2010; Kitagawa et al., 2006; Claesson et al., 2004; Esposito et al., 2001; Curry et al., 1994).

In 2016-2017, the most severe seismic sequence in Italy since the 1980 Irpinia earthquake hit a wide area of Central Italy comprising large parts of the Lazio, Marche, Abruzzi and Umbria regions. Three main shocks of Mw 6.1 (August 24th, 2016, epicenter near Accumoli), 5.9 (October 26th, 2016, epicenter near Visso) and 6.5 (October 30th, 2016, the strongest event, with epicenter near Norcia) occurred (Chiaraluce et al., 2017). The latter two events produced the main effects (e.g., Rossi et al., 2019; Gori et al., 2018; Barberio et al., 2017; Galli et al., 2016) in the Sibillini Mts. Range and partially in the high valley of the Tenna River area. A suite of geological effects took place, among which most notable was the extensive pattern of coseismic ruptures along the Vettore Mt.- Bove Mt. Fault System, with surface offset locally reaching 2 meters (e.g., Testa et al., 2019; Civico et al., 2018; Ferrario and Livio, 2018; Villani et al., 2018; Smeraglia et al., 2017).

The coseismic effects on groundwater resources induced by the 2016-2017 Central Italy seismic sequence were registered in many sites all around the Sibillini Mts. region and affected spring and water-course discharges and groundwater heads levels (e.g., Di Matteo et al., 2020; Fronzi et al., 2020; Valigi et al., 2020a, 2020b, 2019; Martarelli et al., 2020; Petitta et al., 2018). There was also a great impact on the groundwater dynamics of the fissured carbonate aquifers (e.g., Mastrorillo et al., 2023, 2020; Cambi et al., 2022; Mammoliti et al., 2022; Fronzi et al., 2021, 2020; Viaroli et al., 2021; Rosen et al., 2018).

During the first six months of the seismic sequence, in an area located within 100 km of the epicentral zone and characterized by fractured carbonate aquifers, an increase of about 10 $m^3/s$ of spring and river discharge was estimated and corresponds to more than 0.1 $km^3$ of groundwater release. The most probable reason for these anomalies was due to an increase of the bulk hydraulic conductivity within the aquifers, causing rise of hydraulic levels in the basal discharge areas and, conversely, a consequent level fall in some recharge areas (Petitta et al.,

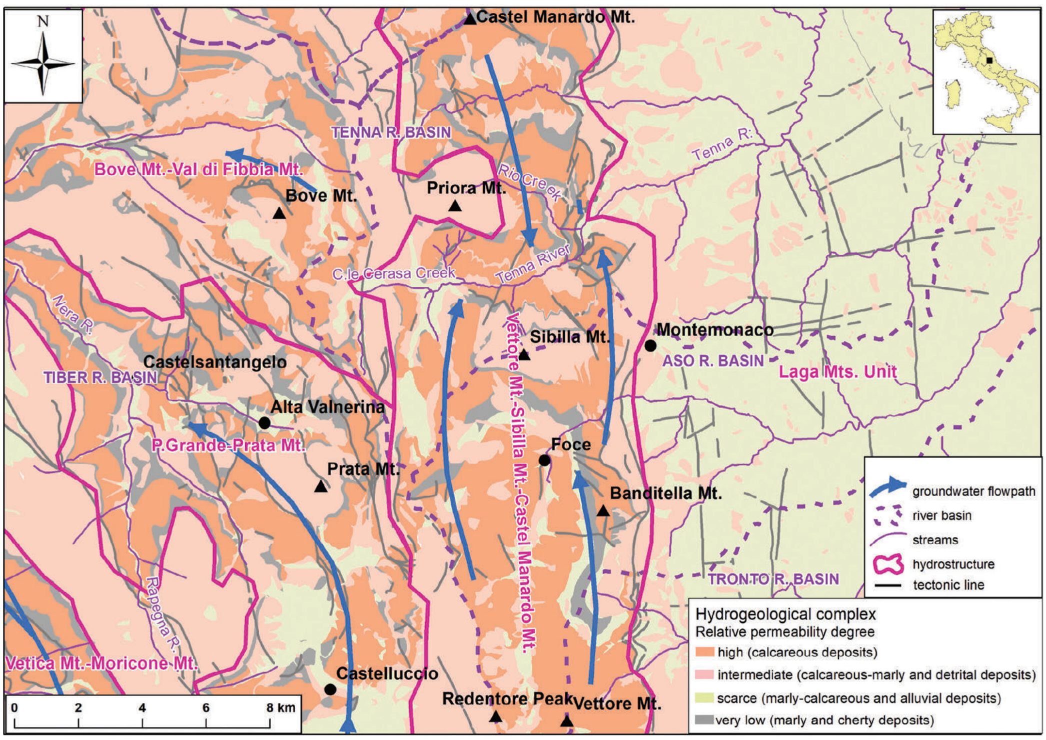


*Fig. 1 - Hydrogeological setting at large scale around the study area (modified from Martarelli et al., 2020). Inset map shows study area location in the Italian context. Geographical coordinates of the NW and SE edges of the figure are lat.42.980°, long.13.080° and lat.42.820°, long.13.420°, respectively.*

Fig. 1 - Inquadramento idrogeologico dell'area vasta nell'intorno dell'area di studio (modificato da Martarelli et al., 2020). Nell'inserto a piccola scala è indicata l'ubicazione dell'area di studio nell'ambito del territorio italiano. Le coordinate geografiche degli spigoli NW e SE della figura sono, rispettivamente, lat.42.980°, long.13.080° e lat.42.820°, long.13.420°.

 DOI 10.7343/as-2026-946

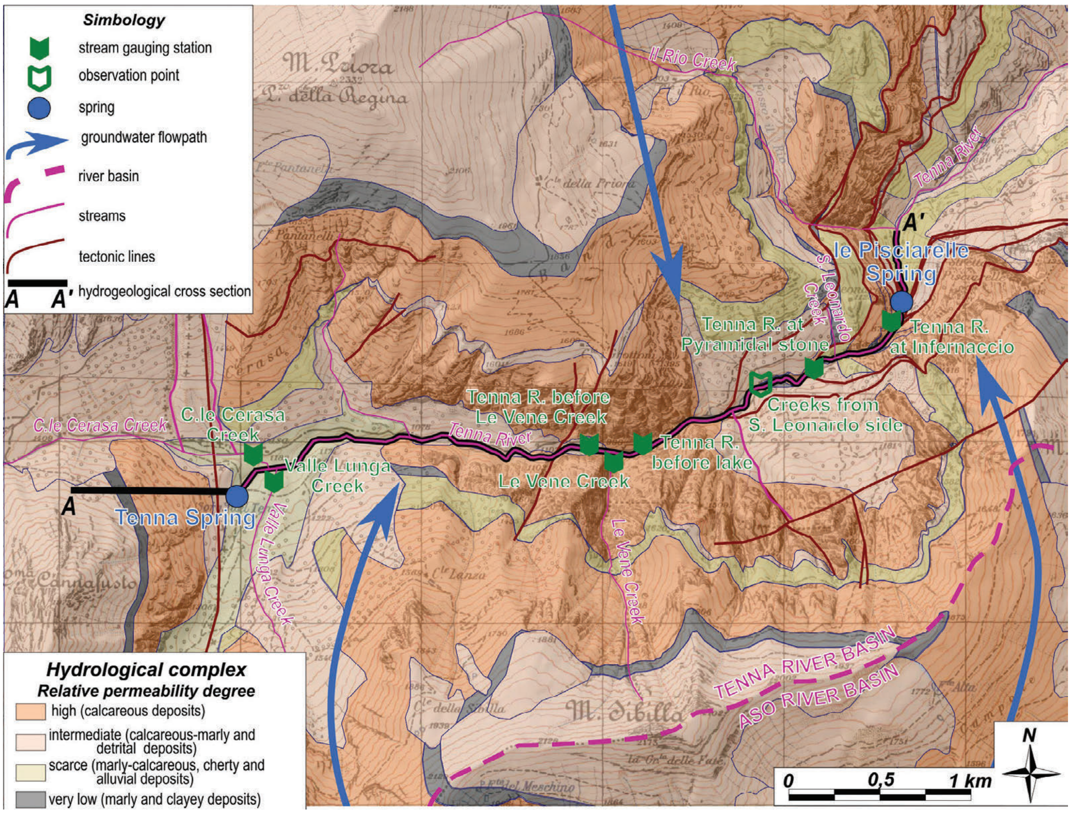


*Fig. 2 - Hydrogeological simplified sketch map of the study area (modified from Martarelli et al., 2020) showing the location of the control points. The location of 2D hydrogeological sketch (reported in Fig. 4) is here shown. Geographical coordinates of the NW and SE edges of the figure are lat.42.940°, long.13.220° and lat.42.890°, long.13.320°, respectively.*

Fig. 2 - Schema idrogeologico semplificato dell'area di studio (modificato da Martarelli et al., 2020) con l'ubicazione dei punti di controllo. È riportata la traccia dello schema 2D di Fig. 4. Le coordinate geografiche degli spigoli NW e SE della figura sono, rispettivamente, lat.42.940°, long.13.220° e lat.42.890°, long.13.320°.

2018). Shaking, compression and aquifer boundary breaking effects likely occurred as well (Petitta et al., 2018).

In the context of a research agreement with the Sibillini Mts. National Park, the Geological Survey of Italy of ISPRA (Italian Institute for Environmental Protection and Research) started in June 2018 hydrogeological surveys aimed to evaluate the possible near-field coseismic effects of the cited seismic sequence on the temporal variation of groundwater resources in some sites of this area. One of these sites was the high valley of the Tenna River (Figs. 1 and 2).

The present paper proposes a discussion on the spatial and seasonal pattern of groundwater–surface water exchanges post-earthquake, on the evidence of recovery by summer 2020 and on the role of lithostratigraphic thresholds.

With respect to previous studies on the hydrogeological effects of the 2016-2017 seismic sequence in the Sibillini Mts., the main contribution of this paper is the reconstruction of a local conceptual model, the analysis of groundwater-surface water exchanges along the Tenna River, and the identification of elevation sectors with different hydraulic behavior.

## Materials and methods

### *Geological and hydrogeological settings*

The Sibillini Mts. area is in the central sector of the Apennine fold and thrust belt and consists of Meso-Cenozoic rocks referred to the Umbria-Marche Succession (e.g., Pierantoni et al., 2013; Centamore and Deiana, 1986; Centamore et al., 1971; Figs. 1 and 2). Hettangian-Sinemurian shallow-water, massive carbonates accumulated in a peritidal carbonate platform represent the oldest deposits cropping out in the study area (Calcare Massiccio formation – MAS). These carbonates are followed by Sinemurian to Burdigalian well-bedded pelagic and hemipelagic deposits (2500-3000 m of total thickness). Middle Miocene-Pliocene hemipelagic and siliciclastic deposits featured by facies and thickness variations accumulated in a foreland basin-wedge top basin depositional setting, and close the marine sedimentary cycle, in turn followed by Pleistocene continental deposition. This succession records polyphasic deformations, from the Early Jurassic Tethyan rifting to the Late Miocene orogenic compression, and to the Quaternary post-orogenic extension (e.g., Curzi et al., 2024; Santantonio et al., 2024, 2022; Cipriani et al., 2020a, 2020b; Cipriani, 2019, 2016; Pierantoni et al., 2013; Deiana and Pialli, 1994; Calamita and Deiana, 1988; Calamita et al., 1982).

As concerns the groundwater resource scenario, the calcareous fissured and karstified lithotypes characterizing the Central-Northern Apennine display a high effective infiltration grade (from 500 to 700 and up to 900 mm/yr, respectively in the Umbria-Marche and Lazio-Abruzzi aquifers) and in total feed a groundwater yield of about 300 $m^3/s$ (Petitta et al., 2018; Barberio et al., 2017; Boni et al., 2010, 1986). The Miocene-Pliocene syn-orogenic silici-clastic deposits act as an aquitard (Petitta et al., 2018, 2011; Barberio et al., 2017). The Sibillini Mts. fissured and subordinately karstified carbonate ridge hosts main aquifers feeding perennial springs having, in general, a constant flow rate and linear streambed features, as along the Tenna River, or are located at the margins of those aquifers (e.g., Di Matteo et al., 2020; Fronzi et al., 2020; Boni et al., 1986).

In situ permeametry conducted parallel to bedding and orthogonal to bedding on poorly deformed calcareous (Maiolica and Scaglia Rossa formations) and marly (Marne a Fucoidi formation) lithotypes of Sibillini Mts. provided permeability mean values ranging from ~$2\times10^{-2}$ D and ~$7\times10^{-3}$ D, with the lower values coincident with the marly deposits orthogonal to bedding (Curzi et al., 2024). Thrusts act as hydraulic barrier as well, especially if they involve clay-rich rocks, as recently described by Curzi et al. (2024) for the Sibillini Mts. Thrust. Permeability measured in situ orthogonal to principal slip surface of thrusts and S-C tectonites provided values up to ~$3\text{x}10^{-5}$ D (Curzi et al., 2024).

The complex tectonic processes that occurred in the study area induced the differentiation of the Sibillini Mts. ridge in several hydrogeological units (e.g., Viaroli et al., 2021; Fronzi et al., 2020; Nanni et al., 2020; Boni et al., 2010). According to the present paper and Martarelli et al. (2020), the hydrogeological unit which the high valley of the Tenna River is located in (Vettore Mt.-Sibilla Mt.-Castel Manardo Mt. Unit; Fig. 1) is composed of calcareous, calcareous-marly, marly-calcareous, marly and cherty, alluvial and detrital deposits. Figures 1 and 2 also show that the Basal Calcareous Aquifer at the Tenna River area is fed by waters mainly coming from Castel Manardo Mt., in the north, but also subordinately from the Sibilla Mt., in the south. This latter relief is partially hydraulically connected to the Vettore Mt. area, further in the south (Valigi et al., 2020a; Nanni et al., 2020).

According to the previously cited literature (e.g., Martarelli et al., 2020; Boni et al., 1986; Boni and Bono, 1982) and to the outcomes of the present study, the terrains cropping out in the high valley of the Tenna River may be grouped in the following hydrogeological complexes (Figs. 1 and 2; acronyms composed of three capital letters represent the reference geological formations; effective infiltration, EI, are from Boni et al., 1986): (i) basal calcareous complex, characterized by high relative permeability grade and constituted by the Lower Jurassic shallow seawater and pelagic carbonates of Calcare Massiccio (MAS) and Corniola (COI) formations. This complex hosts a highly productive basal regional aquifer (Basal Calcareous Aquifer, maximum thickness 600-800 m, sustained by the underlying evaporitic deposits of the Anidriti di Burano formation (ADB), maximum total thickness 500-700 m in boreholes), EI of the calcareous deposits is higher than 800 mm/yr; (ii) upper calcareous complex characterized by high relative permeability grade, constituted by the uppermost Jurassic-Lower Cretaceous deposits of Maiolica formation (MAI). It hosts a main calcareous aquifer (Maiolica Aquifer, thickness 200-250 m, sustained by the underlying calcareous-cherty-marly aquitard-aquiclude composed of Marne di Monte Serrone – RSN – and involving the Middle-Upper Jurassic (Calcari e Marne a Posidonia and Calcari Diasprigni formations), total thickness 150-250 m). When involved in tectonic processes, the Middle-Upper Jurassic carbonates, generally exhibiting a scarce permeability, may host up to 200 m thick locally relevant aquifer (MUJ) sealed by the underlying aquiclude of Marne di Monte Serrone formation (RSN). The EI of calcareous deposits is higher than 800 mm/yr (the EI of MUJ is generally lower than 400 mm/yr); (iii) calcareous-marly complex, characterized by intermediate relative permeability grade. This complex involves Upper Cretaceous-Eocene (Scaglia s.l. formation – SAA) deposits. It hosts a relatively significant aquifer, as the Scaglia Aquifer, whose thickness can reach 200-300 m, sustained by the underlying marly aquiclude of Marne a Fucoidi formation (FUC, thickness 30-50 m). The EI of calcareous-marly deposits is 500-600 mm/yr; (iv) marly-calcareous and marly complex (total thickness about 200 m), characterized by scarce relative permeability grade. In the study area it is represented by the Oligocene hemipelagic deposits of Scaglia Cinerea (SCC, Upper Eocene-Oligocene). This complex lacks significant aquifers and its EI varies from 200 to 300 mm/yr (less than 200 mm/yr in the marly terranes); (v) detrital deposit complex, intermediate relative permeability grade. In the study area, it is characterized by Quaternary coarse grained, matrix-poor, poorly to not-cemented, slope and scree deposits, and it may host subordinate aquifers (total thickness up to some tenths of meters), EI varies from 300 to 500 mm/yr; (vi) alluvial deposit complex (thickness up to some tenths of meters), scarce relative permeability grade. In the study area, it is characterized by Quaternary matrix-supported gravels, and it hosts the alluvial plain unconfined aquifer, EI is less than 200 mm/yr.

It was envisaged (e.g., Cambi et al., 2022; Mammoliti et al., 2022; Mastrorillo et al., 2020) that the most probable origin of the groundwater resources at the valley of the Tenna River is from the Basal Calcareous Aquifer at the NE sector of the Sibillini Mts.. Thus, according to the "basins in series" conceptual model (Mastrorillo et al., 2020), the most exhaustive model for the understanding of the interaction between Sibillini Mts. hydrogeological units, the Tenna River sector, located at the NE part of the Sibillini Mts., suffered a relative water shortage, due to a partial transfer of groundwater towards other southwestern hydrogeological units. These implications were also defined in some previous studies within the Sibillini Mts. Range (e.g., Mastrorillo et al., 2023; Cambi et al., 2022; Mammoliti et al., 2022; Fronzi et al., 2021; Viaroli et al., 2021). Following these Authors and according to geostructural, artificial water tracing test, discharge, geochemical, and isotope evidences, it was pointed out that, in carbonate aquifers, a post-seismic discharge increase is often attributed to an increase of bulk permeability and diversion of groundwater due to co-seismic fracturing. In the Sibillini Mts. context, the main NNW-directed groundwater flow was diverted to the west, a discharge deficit was observed at the footwall of the activated fault system, while a conversely relevant discharge increase, accompanied by geochemical variations, occurred at the hanging-wall fault system. These studies also highlighted that the seismic sequence temporarily changed the behaviour of the normal faults, which act predominantly as barriers to flow in the interseismic period, and water flow was normally favoured along the fault strikes. On the contrary, during earthquakes, groundwater flow can be significantly diverted perpendicularly to fault-strikes due to co-seismic fracturing and consequently permeability increase. Furthermore, springs on the western flank of the Sibillini Mts. exhibited increased discharge, whereas those on the eastern flank suffered a pronounced reduction in their groundwater discharge.

## Methods

The present study has been carried out by means of field activities (stream gauging and physical-chemical parameter measurements) according to quantitative hydrogeological method (e.g. Mastrorillo et al., 2009; Boni et al., 1986; Boni and Bono, 1982). Following this criterion, the reciprocal hydraulic exchanges between groundwater (GW) and surface water (SW) and the consequent identification of streambed springs have been estimated by discharge measurements conducted in sequence along streams during low-water periods. The scenario has been confirmed also in high-water periods. The emitted discharges have been calculated by difference between the water amounts measured in consecutive gauging stations along streambed and balanced considering the in and out contributions by tributaries and/or derivations (Boni and Ruisi, 2002).

The field activities, the technical instruments used, and the applied methods are here listed and then described in the following subsections: (i) stream flow measurements; (ii) in situ hydrochemical measurements; (iii) GW and SW reciprocal hydraulic exchange characterization; (iv) geological and hydrogeological characterization; (v) climatic characterization.

Stream flow measurements have been conducted using an electromagnetic induction flowmeter OTT Nautilus C2000 fixed on a centimetric graduated rod. The hydraulic flow speed data are directly obtained at each speed measurement point within a calibrated grid at the selected cross section, including about ten points per square meter. The specified tolerance of the measured values is within 1% of the measured value (±2 mm/s). In any case, also considering the variability with time and space of natural stream flow and of real hydraulic condition within flow section, a total measurement operating error may be estimated in less than 10% referred to each individual discharge measurement. The stream discharge values have been computed by a software that performs flow speed integral calculations along each vertical and then horizontal arrangements of grid measure points.

Reciprocal exchanges between groundwater and surface water were characterized for each monthly field campaign by calculation of the hydraulic budget along water courses, in term of both drainage (water from aquifer to stream; increasing discharge values from high to low stream course gauging station) or loss (water from stream to aquifer; decreasing discharge values from high to low stream course gauging station), according to Boni and Ruisi (2002) method. Calculation, as already mentioned, was based on the measured discharge values at seriate gauging stations along streams and related tributaries. Examples concerning the campaigns in June and August 2018 were reported in table 1, while a map with gauging site locations is shown in Figure 2. Accordingly, the time variations of groundwater resources were estimated to have, whenever possible, indications on the probable evolution of these resources in the short-medium term. The results of the calculation of drainage/loss of discharge along riverbed were not considered when they were below the order of magnitude of the discharge operating measurement errors (discharge variation from high to low stream course gauging station is less than about 10% of each individual discharge measurement).

The interaction processes occurring along hydraulic pathways between waters and rocks can be understood by the hydrochemical characterization of groundwater. Then, in situ hydrochemical measurements (electrical conductivity, temperature and pH) have been performed using a field handheld digital multimeter WtW Multi 340i (electrical conductivity: range 0÷1999 μS/cm, resolution 1 μS/cm, precision ±0.5%; temperature: range -5÷105 °C, resolution 0.1 °C, precision ±0.1%; pH: range -2.00÷19.99; resolution 0.01; precision ±0.01).

A collection of available information from other institutions involved in the study of coseismic effects on the groundwater resources of the Sibillini Mts. area (e.g., Umbria and Marche Regions; Central Italy Authority for the Hydrographical District of Central Italy; National Research Council, CNR; National Institute of Geophysics and Volcanology, INGV; Roma La Sapienza, Roma Tre, Perugia, Urbino, Marche and Camerino Universities) preceded the field activities. The related data collected were useful for the definition of a knowledge framework of the reference pre-seismic hydrogeological scenario and for comparison with and verification respect to data collected during the present study (e.g., data available from Marche Region; Valigi et al., 2019; Petitta et al., 2018; Villani et al., 2018).

The geological information used for this study derives from a field mapping project involving the high the Tenna River valley, performed at 1:10,000 scale in 2018 and 2019. The related geological map is partially published in Curzi et al. (2024) and partially still unpublished (Cipriani & Curzi, ISPRA, Geological Map of the Priora Mt.-Sibilla Mt. area, submitted to Geological Field Trips & Maps, 2026).

Hydrogeological surveys aimed at the characterization of the recovery stage after near-field effects of the 2016-2017 Central Italy seismic sequence on groundwater resources started in June 2018 and were carried out by monthly/bimonthly monitoring frequency until July 2020 (about two hydrological years). They included stream discharge and

*Tab. 1 - Examples of calculation of drainage/loss of discharge along riverbeds in the study area, according to Boni and Ruisi (2002) approach (only June and August 2018 field campaigns are reported). In green, calculated values agree with streambed drainage processes; in red, they denote a streambed loss; in black, values are lower than the order of magnitude of the discharge measurement error (less than about 10%).*

Tab. 1 - Esempi di calcolo di drenaggio/perdita di portata in alveo nell'area d'indagine utilizzando il criterio di Boni e Ruisi (2002) (sono stati riportati solo i risultati delle campagne di misura di giugno e agosto 2018). In verde, i valori calcolati portano a considerare processi di drenaggio in alveo; in rosso, essi evidenziano una perdita in alveo; in nero, i valori sono al di sotto dell'ordine di grandezza dell'errore della misura (meno del 10% circa).

| | | | | June 2018 field survey | | | | August 2018 field survey | | | |
|---|---|---|---|---|---|---|---|---|---|---|---|
| Monitoring station name | | Elev. a.s.l. (m) | Draining/ dispersant streambed length (km) | Tributary streams ($m^3/s$) | Tenna River ($m^3/s$) | Streambed Drainage or Loss ($m^3/s$) | Streambed Drainage or Loss/km (L/s/km) | Tributary streams ($m^3/s$) | Tenna River ($m^3/s$) | Streambed Drainage or Loss ($m^3/s$) | Streambed Drainage or Loss/km (L/s/km) |
| 1 | C.le Cerasa Creek | 1178 | | | | | | 0.000 | | | |
| 2 | Valle Lunga Creek + Tenna Spring (overflow) | 1175 | | | 0.019 | | | | 0.000 | | |
| 3 | Tenna Spring (overflow) | 1178 | | | 0.028 | | | | 0.000 | | |
| | Water exchange calculation: 2-3 | | 0.2 | | | -0.009 | -45 | | | 0.000 | 0 |
| 4 | Tenna River after C.le Cerasa Creek (calculation:1+2) | 1175 | | | 0.194 | | | | 0.000 | | |
| 5 | Tenna River before Vene Creek | 990 | | | 0.873 | | | | 0.198 | | |
| | Water exchange calculation: 5-4 | | 1.8 | | | 0.679 | 377 | | | 0.198 | 110 |
| 6 | Vene Creek | 990 | | 0.072 | | | | 0.001 | | | |
| 7 | Tenna River after Vene Creek (calculation: 5+6) | 990 | | | 0.945 | | | | 0.199 | | |
| 8 | Tenna River before lake | 985 | | | 0.802 | | | | 0.208 | | |
| | Water exchange calculation: 8-7 | 970-945 | 0.3 | | | -0.143 | -477 | | | 0.009 | 30 |
| 9 | Creeks from S. Leonardo side | 945 | | *0.020* | | | | 0.010 | | | |
| 10 | Tenna River after San Leonardo side (calculation: 8+9) | 941 | | | *0.822* | | | | *0.218* | | |
| 11 | Tenna River at pyramidal stone | | | | 0.900 | | | | *0.184* | | |
| | Water exchange calculation: 11-10 | | 1 | | | 0.078 | 78 | | | -0.034 | -34 |
| 12 | Tenna River al Infernaccio wade | 845 | | | 0.802 | | | | *0.197* | | |
| | Water exchange calculation: 12-11 | | 0.6 | | | -0.098 | -163 | | | 0.013 | 22 |
| 13 | Le Pisciarelle springs | 925-845 | | *0.020* | | | | *0.010* | | | |

hydrochemical measurements of groundwater (temperature, T; specific electrical conductivity, EC; pH). All monitoring points were measured during the following field campaigns: June, August, and October 2018; March, April, May, July, August, September, October, November, and December 2019; June and July 2020.

Climatic characterization by analysis of available meteoclimatic long-term datasets (from 1989 to 2019; precipitation - also snow, at the stations equipped with snow-gauges - and air temperature) at selected stations located all around the study area were performed (Table 2). Data were downloaded from websites of Centro Funzionale Multirischi della Protezione Civile della Regione Marche (Regione Marche, 2022), Servizio Idrografico della Regione Umbria (Regione Umbria, 2022), Servizio Idrografico della Regione Lazio (Regione Lazio, 2022) and Annali Idrologici (1900-2012). Snow depth was converted into water equivalent considering the influence of the wind and other accidents during measurements and the estimation of snow density mainly based on air temperature and humidity and wind speed according to, e.g., Helfricht et al. (2018), Lendvai et al. (2015), Cugerone et al. (2012). The method used to compute climatic characterization is based on spatial query analyses in GIS environment, which enables the transformation of raw data into operational information as spatial relationships, patterns, trends. Furthermore, with respect to the study area, due to its vicinity, comparable elevation and exposition to the high valley of the Tenna River, the best representative local station is at Montemonaco. The station at Montemonaco (data from 1951-2022) was selected as well for carrying out a non-parametric Mann-Kendall test (Sneyers, 1990; Kendall et al., 1983), to evidence any possible statistical trend for rainfall and air temperature series.

The meteoclimatic features of the Sibillini Mts. Range were defined by daily and monthly rainfall and air temperature time series available at 33 meteoclimatic gauging stations (among them 30 and 19 were feasible for rainfall and temperature characterization, respectively) situated among Umbria, Marche and Lazio regions (elevation a.s.l. between 390 m, Montedinove, and 1917 m, Monte Bove Sud; Table 2). Available data were qualitatively evaluated to evidence the occurrence of lacking or too short time series and, if necessary, a reconstruction of the value gaps by multiple regression method was performed. Multiple regression was used to reconstruct missing data in rainfall stations with at least 60% data coverage over the last 30 years, considering as predictors only stations with a multiple coefficient of determination $R^2 \geq 0.8$. The low number of stations and the lack of data for elevation over 1500 m a.s.l. lead to the necessity of creating fictitious stations based on calculation of mean rainfall vs. elevation gradient. The estimation of rainfall at fictitious stations was performed using interpolation and elevation correction based on mean precipitation-elevation gradients (Roquier et al., 2022; Fiddes et al., 2020; Berne and Uijlenhoet, 2009). Evapotranspiration has been calculated according to Turc (1961) method.

Table 3 shows reference geographical coordinates and elevation of the control points selected within the study area. They include one spring and nine streams measured by flowmeter gauging stations.

It is finally noteworthy to advise that it was not possible to reach the Capotenna Plain, and then the field campaigns were not conducted, between November 2018-February 2019 and January-February 2020, due to permanence of snow and the related unsafe conditions, and between March-May 2020, according to Covid-19 sanitary restrictions and journey limitations. The lack of field campaign data during these

*Tab. 2 - Thermo-pluviometric stations available for the meteo-climatic characterization of the study area (data from Regione Marche, 2022, Regione Umbria, 2022; Regione Lazio, 2022). The annual mean air temperature ($T_a$) has been calculated on data from time series of at least 10 years, while annual mean rainfall (P) values are based on 30-year time series (1989-2019), partially reconstructed by multiple regression method, when necessary. Annual mean P is in bold if it includes snow depth.*

Tab. 2 - Elenco delle stazioni utilizzate per la caratterizzazione meteoclimatica dell'area di studio (dati da Regione Marche, 2022, Regione Umbria, 2022; Regione Lazio, 2022). La temperatura dell'aria ($T_a$) media annua è stata calcolata sulle serie temporali di lunghezza minima di 10 anni, mentre la precipitazione (P) media annua è stata ottenuta sulle serie trentennali (1989-2019), parzialmente ricostruite mediante regressione multipla, quando necessario. La precipitazione media annua è in grassetto se include l'altezza della neve.

| Station name | Elev. (m a.s.l.) | Annual mean $T_a$ (°C) | Annual mean P (mm) | Station name | Elev. (m a.s.l.) | Annual mean $T_a$ (°C) | Annual mean P (mm) |
|---|---|---|---|---|---|---|---|
| Acqusanta Terme | 392 | ---- | 970 | Monte Cavallo | 960 | 11.6 | 1264 |
| Accumuli ARSIAL | 1171 | 10.3 | 1115 | Montedinove | 390 | 15.8 | --- |
| Amandola | 468 | --- | 1068 | Montefortino Assan | 772 | 11.7 | 1156 |
| Amatrice | 955 | --- | 955 | Monteleone di Spoleto | 935 | 10.4 | 1119 |
| Arquata del Tronto | 720 | --- | 1151 | Montemonaco | 995 | 11.6 | 1117 |
| Capodacqua | 842 | 11.0 | 1092 | Norcia | 700 | 12.0 | 806 |
| Cascia | 626 | 11.7 | 877 | Pievebovigliana | 451 | --- | 941 |
| Castelsantangelo-Nerea | 720 | 10.3 | 1218 | Pintura di Bolognola | 1360 | 9.2 | 1428 |
| Croce Casale | 657 | --- | 927 | Ponte Tavola | 832 | --- | 1086 |
| Endesa Visso | 753 | --- | 1191 | Sarnano Assan | 480 | --- | 1080 |
| Fiastra Trebbio | 747 | 11.7 | 1207 | Sassotetto | 1365 | 9.0 | --- |
| Fiume Fiastra | 618 | --- | 1232 | Sellano | 608 | 12.1 | 928 |
| Forsivo | 792 | --- | 835 | Serravalle in Chienti | 754 | 10.6 | 939 |
| Gelagna Alta | 711 | --- | 1057 | Santa Maria Pieca | 467 | --- | 1028 |
| Illice | 706 | --- | 936 | Umito | 646 | 12.1 | --- |
| Monte Bove sud | 1917 | 5.9 | **841** | Ussita | 749 | 10.5 | 1057 |
| Monte Prata | 1813 | 6.2 | **965** | | | | |

*Tab. 3 - Geographical coordinates in WGS84 system and reference elevation of the main selected monitoring stations.*

Tab. 3 - Coordinate geografiche nel sistema WGS84 e quote di riferimento delle principali stazioni di controllo selezionate.

| Monitoring station | Latitude | Longitude | Elev. (m a.s.l.) |
|---|---|---|---|
| Tenna Spring (overflow) | 42°54'46"N | 13°14'14"E | 1178 |
| C.le Cerasa Creek | 42°54'48"N | 13°14'11"E | 1178 |
| Tenna River after Valle Lunga Creek | 42°54'46"N | 13°14'17"E | 1175 |
| Tenna River after Vene Creek | 42°54'49"N | 13°15'41"E | 990 |
| Tenna River before lake | 42°54'51"N | 13°15'44"E | 985 |
| Tenna River after San Leonardo side | 42°55'05"N | 13°16'22"E | 945 |
| Tenna River at pyramidal stone | 42°55'08"N | 13°16'27"E | 941 |
| Tenna River al Infernaccio wade | 42°55'17"N | 13°16'46"E | 845 |
| Creek from S. Leonardo side | 42°55'04"N | 13°16'14"E | 970-945 |
| Le Pisciarelle Springs | 42°55'19"N | 13°16'47"E | 925-845 |

months, with respect to the whole monitoring period, was not significant and has not likely affected the interpretation of the seasonal and post-seismic evolution.

## Results and discussion

Complete set of data collected during this study (e.g., hydrochemical parameters and stream gauging measurements) is available on reasonable request to corresponding author's e-mail address (Table 4).

It is worth noting that the collected time series combines different types of data from different sources and time periods, including Capotenna withdrawal and the Tenna River discharge. Withdrawal data and natural river discharge data are not directly equivalent and were interpreted with due caution.

### *Meteo-climatic scenario*

The calculated mean annual rainfall for the whole range 1951-2022 at the Montemonaco gauging station (elevation 995 m a.s.l.) is about 1117 mm/yr, while the mean annual air temperature is 11.6°C. The monthly air temperature ($T_a$), rainfall (P) and evapotranspiration regimes of three selected post-seismic reference years mostly covering the study period (from 2017 to 2019) are represented in Figure 3. They confirm the inclusion of the study area in the Apennine climatic region. The comparison between $T_a$ and P standardized values, in the same figure, shows that $T_a$, and thus accordingly the strongly directly dependent evapotranspiration values, mainly prevails during June-September ($T_a$ curves are higher than P histograms) and is negligible during other months ($T_a$ curves are in the same order of magnitude of P histograms). It is also evident (Fig. 3) that, at Montemonaco station, worst climatic conditions for effective rainfall increase (strongly directly dependent from P and inversely from $T_a$ values) often occurred: a) in March-August and October 2017, b) in January, April, July, November and December 2018, c) February, March, June, October and December 2019.

The selected time series were tested by Mann-Kendall method (Sneyers, 1990; Kendall et al., 1983) for evidencing

*Tab. 4 - Summary of the mean, maximum and minimum values of the hydrochemical parameters of the main selected control points (the number of collected measurements is reported between square brackets after the names).*

Tab. 4 - Tabella riassuntiva dei valori medi, massimi e minimi dei parametri idrochimici dei principali punti di controllo selezionati (tra parentesi quadre dopo il nome è indicato il numero di misure effettuate).

| Name | Stream | Elevation m a.s.l. | EC µS/cm | | | $T_{H_2O}$ °C | | | pH | | |
|---|---|---|---|---|---|---|---|---|---|---|---|
| | | | mean | max | min | mean | max | min | mean | max | min |
| C.le Cerasa Creek [1] | C.le Cerasa | 1178 | 211 | ----- | ----- | 8.3 | ----- | ----- | 8.2 | ----- | ----- |
| Tenna Spring (overflow) [13] | Capotenna | 1178 | 219 | 224 | 212 | 9.0 | 15.6 | 4.6 | 7.7 | 8.3 | 7.1 |
| Valle Lunga Creek + Tenna Spring [1] | Valle Lunga | 1175 | 217 | ----- | ----- | 7.1 | ----- | ----- | 7.8 | ----- | ----- |
| Tenna River after Vene Creek [14] | Tenna | 990 | 231 | 254 | 219 | 7.5 | 9.7 | 5.3 | 7.6 | 8.1 | 7.2 |
| Vene Creek [9] | Le Vene | 990 | 209 | 231 | 176 | 7.5 | 13.1 | 1.9 | 7.5 | 7.9 | 7.2 |
| Tenna River before lake [14] | Tenna | 985 | 229 | 243 | 214 | 7.7 | 9.6 | 5.4 | 7.6 | 8.2 | 7.2 |
| Creek from S. Leonardo side [7] | S. Leonardo | 970-945 | 275 | 282 | 268 | 8.8 | 11.0 | 7.9 | 7.6 | 7.8 | 7.3 |
| Tenna River at pyramidal stone [13] | Tenna | 941 | 240 | 255 | 222 | 8.2 | 11.6 | 4.8 | 7.7 | 8.2 | 7.3 |
| Spring at pyramidal stone right [1] | Tenna | 941 | 261 | ----- | ----- | 8.0 | ----- | ----- | 7.9 | ----- | ----- |
| Tenna River al Infernaccio wade [10] | Tenna | 845 | 239 | 247 | 222 | 8.2 | 11.6 | 4.8 | 7.7 | 8.2 | 7.3 |
| Le Pisciarelle Springs [12] | Pisciarelle | 925-845 | 246 | 252 | 239 | 11.4 | 17.3 | 4.5 | 7.6 | 8.1 | 7.3 |

DOI 10.7343/as-2026-946

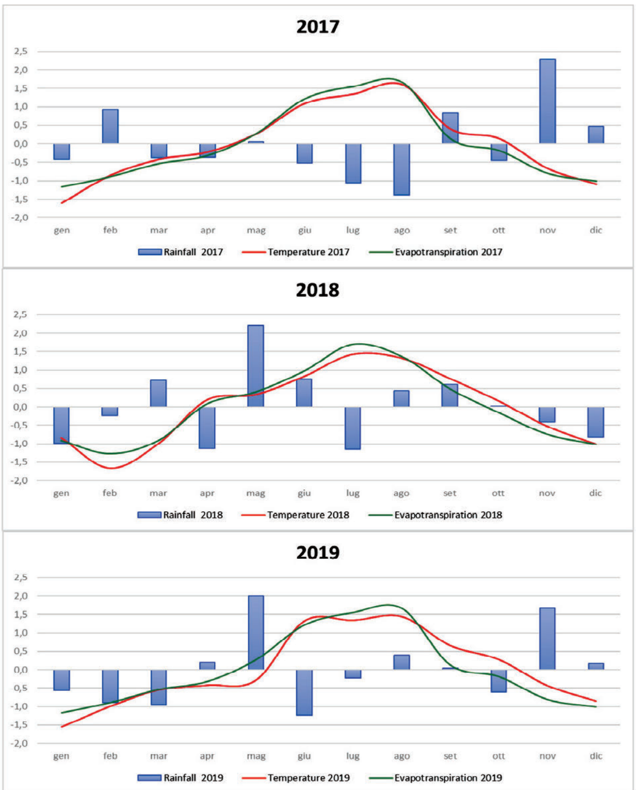


*Fig. 3 - Thermo-pluviometric regime and evapotranspiration data for the Montemonaco meteoclimatic station (987 m a.s.l.) during the years 2017-2019 of the present study (standardized data from Regione Marche, 2022).*

Fig. 3 - Regime termo-pluviometrico e dati di evapotraspirazione per la stazione meteo-climatica di Montemonaco (987 m s.l.m.) negli anni 2017-2019 del presente studio (dati standardizzati da Regione Marche, 2022).

possible statistical trends. A confidence level for the Mann-Kendall tests was adopted for Z values ±2.2. No significant trends towards a positive or negative variation of the total rainfall (trend value of Mann-Kendall Test Z=-1.19; Sen's slope estimate=-1.515) and of January and December rainfall (trend value of Mann-Kendall Test Z=-2.11 and -1.77, respectively; Sen's slope estimate=-0.755 and -0.736, respectively) at Montemonaco station were evidenced. As regards $T_a$, no significant trends related to the increasing of the annual mean values (trend value of Mann-Kendall Test Z=-0.50; Sen's slope estimate=-0.011) were noticed and only the mean values of October and September (trend value of Mann-Kendall Test Z=2.20 and 1.83, respectively; Sen's slope estimate=0.205 and 0.143, respectively) displayed a relative positive trend in the series including 2007-2019 years.

### Conceptual model

The whole of the surveyed hydrogeological results achieved in this research and in a related previous study (Martarelli et al., 2020) allowed the reconstruction of the hydrogeological conceptual model for the study area along a representative rectified cross-section at the high course of the Tenna River (Fig. 4). For the reconstruction of the model, the Tenna River Basin and the hydraulically-related hydrostructures were considered and their borders were assumed as model boundaries. The applicable understandings from the whole collected data were considered. For the reliability and uncertainty assumptions, the approaches of Bredehoeft (2005) and Enemark et al. (2019) were adopted. Some aspects of the model are discussed in the following sections.

### Hydrogeological and hydrological scenario at Capotenna

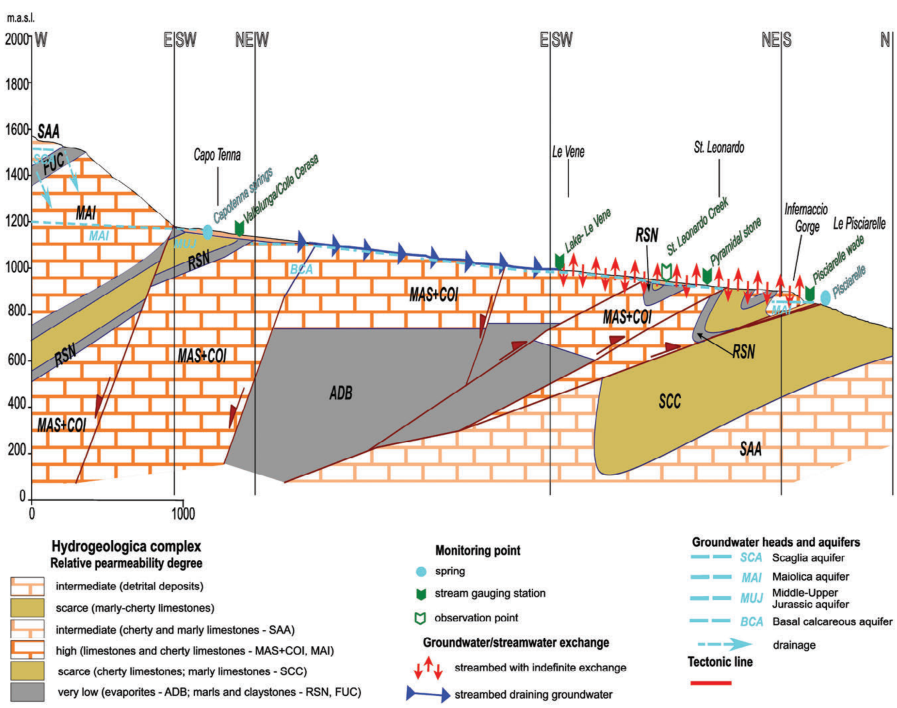


*Fig. 4 - 2D sketch of the hydrogeological asset of the study area along a rectified cross section of the high course of Tenna River (modified from Martarelli et al., 2020). x and y axis scales are not the same. Sketch location is displayed in Figure 2. Acronyms composed of three capital letters in black refer to geological formations and are described within the paragraph dedicated to hydrogeological complexes within "Materials and methods - Geological and hydrogeological settings" section.*

Fig. 4 - Sezione 2D schematica nell'area di indagine lungo una sezione rettificata dell'alveo del Fiume Tenna (modificato da Martarelli et al., 2020). L'asse delle x e quello delle y non hanno la medesima scala. La posizione della traccia dello schema è riportata in Figura 2. Le sigle composte da tre lettere maiuscole in colore nero indicano le formazioni geologiche e sono descritte nel paragrafo dedicato ai complessi idrogeologici nella sezione "Materials and methods - Geological and hydrogeological settings".

During the period June 2018-July 2020, the streams close to the Capotenna Spring sector were wet only in June 2018. Furthermore, the overflow of this spring was active only in the same month (about 30 L/s), in May 2019 (about 20 L/s) and in June-July 2020 (few L/s). The emitted water suddenly infiltered along the streambed in agreement with the role of recharge area played by the Capotenna sector. As evidenced in the hydrogeological rectified cross section along the high course of the Tenna River (Fig. 4), during the remaining part of the monitoring period (July 2018-July 2020), the Maiolica Aquifer, along with the hydraulically connected subordinately relevant MUJ Aquifer, where the former spring has its origin, had not enough hydraulic potential to allow enough flowing of spring water, excluding the tapped water. Only at lower elevation of about 1100 m a.s.l., in correspondence of the Marne di Monte Serrone threshold area, this aquifer was able to pour out overflow water from spring.

Historical measurements of the overflow of the Capotenna Spring are not publicly available. Then, an eventual variation in decreasing of water at the Capotenna plain level cannot be investigated. During the present study the presence of water was only occasionally observed in this area. The lower amount of tapped water at the Capotenna Spring after 2017 summer (Fig. 5 and Table 2) is likely due to variations of the recharge regime of this spring, probably connected with decreasing hydraulic heads within the Maiolica and the connected MUJ and Scaglia Aquifers. As already deduced, this event did not allow an adequate water drainage through the Marne di Monte Serrone low permeable threshold and the overburden alluvial deposits.

## GW-SW exchange by elevation sectors

Along the Tenna River course, in March-May and November-December 2019 and in June 2020, it was apparent (Fig. 5 and Table 5) a progressive discharge increase, corresponding to recovery stages after the low water periods,

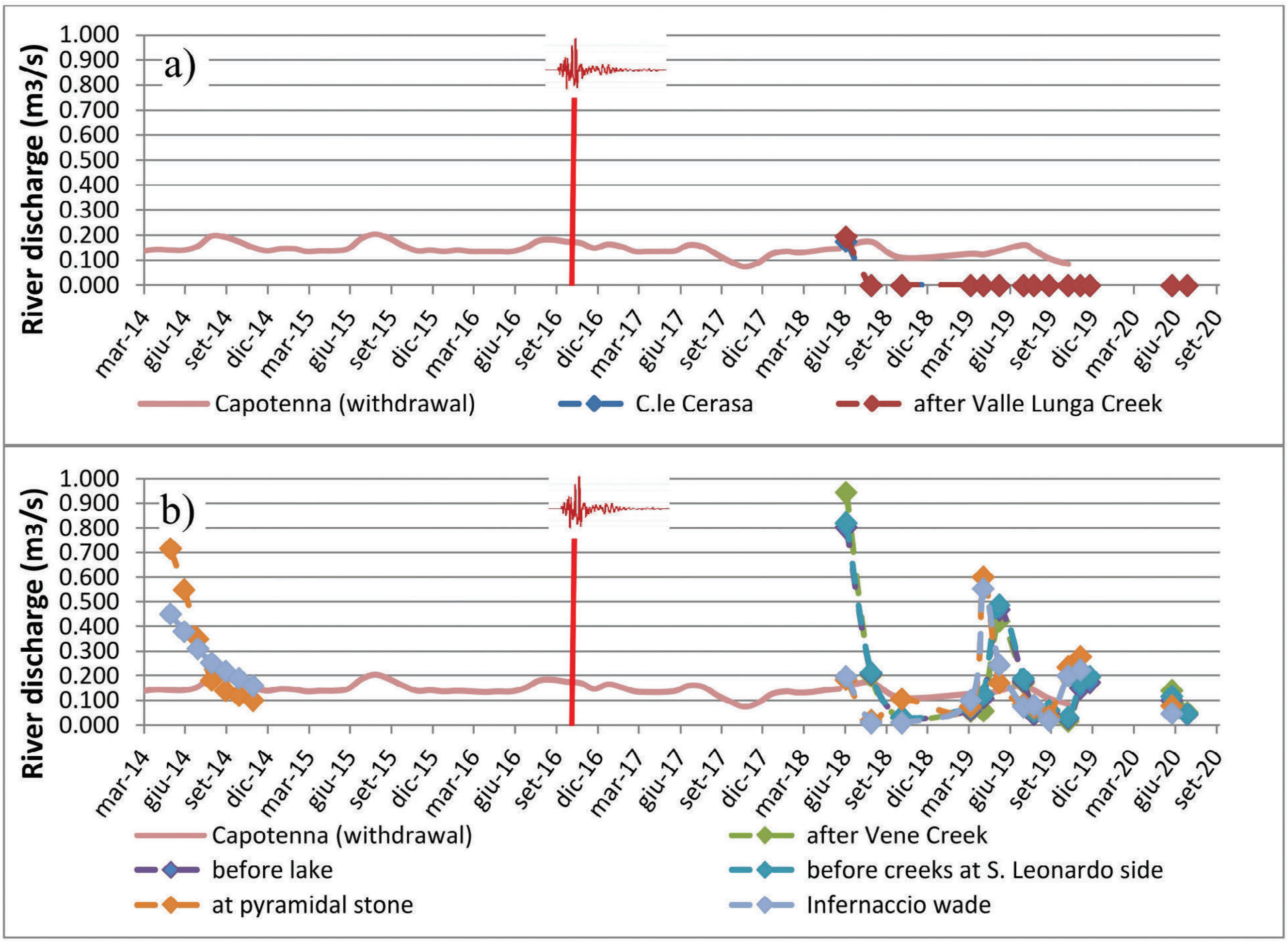


*Fig. 5 - Plot of the discharge variation with time for Capotenna withdrawal (from April 2014 to November 2019; data available from Regione Marche, 2022) and for the Tenna River (data from May to November 2014 are from La Porta et al., 2018; data from June 2018 to July 2020 are from this study) at the control points of the streams of the study area. The main shock event of 30th October 2016 is evidenced by a red line in figure. a) Capotenna sector, 1078-1075 m a.s.l.; b) sector 990-845 m a.s.l..*
*Different types of data from different sources and time periods are here shown.*

Fig. 5 - Diagramma delle variazioni della portata nel tempo del prelievo a Capotenna (da aprile 2014 a novembre 2019; dati disponibili da Regione Marche, 2022) e del corso del Fiume Tenna (i dati da maggio a novembre 2014 provengono da La Porta et al., 2018; i dati da giugno 2018 a luglio 2020 dal presente studio) nei punti di controllo dell'area di studio. Il principale evento sismico del 30 ottobre 2016 è evidenziato dalla linea rossa nella figura. a) Settore di Capotenna, 1078-1075 m s.l.m.; b) settore 990-845 m s.l.m. Differenti tipi di dati di differente origine e intervallo di tempo sono mostrati nella presente figura.

*Tab. 5 - Results of the calculation of streambed drainage/loss of discharges (drainage, in green; loss, in red; unreliable, i.e. lower than about 10% of measured value, in black) measured between the selected gauging stations during the performed field campaigns along the Tenna riverbed. Tenna River yield is also reported.*

Tab. 5 - Risultati del calcolo di drenaggio/perdita di portata in alveo (drenaggio, in verde; perdita, in rosso; inattendibile, i.e. inferiore a circa il 10% della misura, in nero) tra le stazioni di misura oggetto di rilievi di campagna nell'alveo del Fiume Tenna. È stata riportata anche la portata del F. Tenna.

| | | jun-18 | aug-18 | oct-18 | mar-19 | apr-19 | may-19 | jul-19 |
|---|---|---|---|---|---|---|---|---|
| **Water exchange along Tenna River between Tenna Spring and Valle Lunga Creek** | **Tenna River** ($m^3/s$) | 0.028 | 0.000 | 0.000 | 0.000 | 0.000 | 0.020 | 0.010 |
| | Streambed Drainage or Loss ($m^3/s$) | -0.009 | 0.000 | 0.000 | 0.000 | 0.000 | -0.020 | -0.010 |
| | Streambed Drainage or Loss/km (l/s/km) | -45 | 0 | 0 | 0 | 0 | -100 | -48 |
| **Water exchange along Tenna River between C.le Cerasa Creek and Vene Creek** | **Tenna River** ($m^3/s$) | 0.873 | 0.198 | 0.028 | 0.052 | 0.030 | 0.367 | 0.171 |
| | Streambed Drainage or Loss ($m^3/s$) | 0.679 | 0.198 | 0.028 | 0.052 | 0.030 | 0.367 | 0.171 |
| | Streambed Drainage or Loss/km (l/s/km) | 377 | 110 | 16 | 29 | 17 | 204 | 95 |
| **Water exchange along Tenna River between Vene Creek and lake** | **Tenna River** ($m^3/s$) | 0.802 | 0.208 | 0.033 | 0.060 | 0.109 | 0.468 | 0.178 |
| | Streambed Drainage or Loss ($m^3/s$) | -0.143 | 0.009 | 0.005 | 0.003 | 0.051 | 0.046 | 0.006 |
| | Streambed Drainage or Loss/km (l/s/km) | -477 | 30 | 17 | 10 | 170 | 152 | 21 |
| **Water exchange along Tenna River between San Leonardo side and pyramidal stone** | **Tenna River** ($m^3/s$) | 0.900 | 0.184 | 0.020 | 0.105 | 0.076 | 0.601 | 0.172 |
| | Streambed Drainage or Loss ($m^3/s$) | 0.078 | -0.034 | -0.018 | 0.035 | -0.048 | 0.113 | -0.016 |
| | Streambed Drainage or Loss/km (l/s/km) | 78 | -34 | -18 | 35 | -48 | 113 | -16 |
| **Water exchange along Tenna River between pyramidal stone and Infernaccio wade** | **Tenna River** ($m^3/s$) | 0.802 | 0.197 | 0.010 | 0.107 | 0.100 | 0.554 | 0.244 |
| | Streambed Drainage or Loss ($m^3/s$) | -0.098 | 0.013 | -0.010 | 0.002 | 0.024 | -0.047 | 0.072 |
| | Streambed Drainage or Loss/km (l/s/km) | -163 | 22 | -17 | 3 | 40 | -78 | 120 |

| | | aug-19 | sep-19 | oct-19 | nov-19 | dec-19 | Jun-20 | Jul-20 |
|---|---|---|---|---|---|---|---|---|
| **Water exchange along Tenna River between Tenna Spring and Valle Lunga Creek** | **Tenna River** ($m^3/s$) | 0.000 | 0.000 | 0.000 | 0.000 | 0.000 | 0.002 | 0.001 |
| | Streambed Drainage or Loss ($m^3/s$) | 0.000 | 0.000 | 0.000 | 0.000 | 0.000 | -0.002 | -0.001 |
| | Streambed Drainage or Loss/km (l/s/km) | 0 | 0 | 0 | 0 | 0 | -10 | -5 |
| **Water exchange along Tenna River between C.le Cerasa Creek and Vene Creek** | **Tenna River** ($m^3/s$) | 0.078 | 0.040 | 0.016 | 0.102 | 0.169 | 0.109 | 0.050 |
| | Streambed Drainage or Loss ($m^3/s$) | 0.078 | 0.040 | 0.016 | 0.102 | 0.169 | 0.109 | 0.050 |
| | Streambed Drainage or Loss/km (l/s/km) | 44 | 22 | 9 | 57 | 94 | 61 | 28 |
| **Water exchange along Tenna River between Vene Creek and lake** | **Tenna River** ($m^3/s$) | 0.043 | 0.056 | 0.027 | 0.150 | 0.173 | 0.102 | 0.043 |
| | Streambed Drainage or Loss ($m^3/s$) | -0.036 | 0.007 | 0.011 | -0.002 | -0.021 | -0.039 | -0.008 |
| | Streambed Drainage or Loss/km (l/s/km) | -119 | 25 | 37 | -5 | -71 | -129 | -27 |
| **Water exchange along Tenna River between San Leonardo side and pyramidal stone** | **Tenna River** ($m^3/s$) | 0.085 | 0.071 | 0.035 | 0.236 | 0.278 | 0.160 | 0.079 |
| | Streambed Drainage or Loss ($m^3/s$) | 0.033 | 0.010 | 0.003 | 0.066 | 0.080 | 0.043 | 0.033 |
| | Streambed Drainage or Loss/km (l/s/km) | 33 | 10 | 3 | 66 | 80 | 43 | 33 |
| **Water exchange along Tenna River between pyramidal stone and Infernaccio wade** | **Tenna River** ($m^3/s$) | 0.075 | 0.082 | 0.020 | 0.200 | 0.224 | 0.152 | 0.047 |
| | Streambed Drainage or Loss ($m^3/s$) | -0.010 | 0.010 | -0.015 | -0.036 | -0.054 | -0.008 | -0.032 |
| | Streambed Drainage or Loss/km (l/s/km) | -17 | 17 | -25 | -60 | -90 | -13 | -53 |

occurred in October for both the 2018 and 2019 monitored hydrologic years.

During the two-year monitoring period, along the stream course with elevation from 1175-990 m a.s.l., (about 200 m of elevation interval for about 2 km of stream length) an increment of stream discharge of about 0.02-0.68 $m^3/s$, (corresponding to a GW to SW hydraulic contribution of about 10-380 L/s/km; minimum value in low season, maximum in high season) was registered. These waters originated from the Maiolica Aquifer at elevations higher than 1100 m a.s.l. and from the Basal Calcareous Aquifer at relatively lower elevations. The cited low permeable threshold constituted by the Marne di Monte Serrone formations acts as a divide for the contributions coming from the two cited aquifers.

At lower elevations, between 990-985 m a.s.l. (about 5 m of elevation interval for about 300 m of stream length) more limited GW to SW hydraulic contributions occurred (from 0.003-0.05 $m^3/s$; 10-170 L/s/km) but also some decreasing discharge episodes (i.e. a SW to GW hydraulic contribution) happened along Tenna streambed (June 2018, August 2019, November-December 2019, June-July 2020).

The further sectors between 985-945-941-845 m a.s.l. (about 150 m of elevation interval for about 2 km of stream length) evidenced complex hydraulic exchanges from groundwater to surface water and vice versa. These complexities are most likely due to joint effects of (i) 985-945 m a.s.l.: the tectonic fragmentation of carbonate rocks that, at this elevation range, are pervasively deformed by multiple thrust faults interpreted as conjugated structures of the Sibillini Mts. Thrust and the relatively shallow occurrence of the basal, low permeability layer represented by the evaporitic deposits of ADB (Fig. 4; see also Curzi et al., 2024); (ii) 941-845 m a.s.l.: the very shallow occurrence of the low permeability layers represented by the marly deposits of RSN and FUC (Fig. 4). The ADB deposits lie at relatively high structural position, occupying the hanging wall of the Sibillini Mts. thrust resulting in a thinning of the Basal Calcareous Aquifer (Fig. 4).

During the lowest discharge stage in October 2018 and 2019, two dry sectors along the Tenna River were observed (approximately between the elevation of Capotenna at 1178 and 1100 m a.s.l. and between 1070 and 1050 m a.s.l.; Fig. 4). This evidence might be due to exclusively occurrence, during this period of lack of water availability, of streambed flow within alluvial and scree deposits at both the sites (i.e., 1178-1100 and 1070-1050 m a.s.l. elevation ranges).

### *Hydrochemistry and implications*

The hydrochemical parameters (EC, T and pH; Table 4) measured at the control points along the high course of the Tenna River show that mean T values span within a relatively narrow range (7-9°C), while those of the Pisciarelle Springs display mean values of about 11°C. Similarly, the pH values (7.4-8.2 as a whole variation range; slightly to medium alkaline waters) were substantially similar during the different seasonal surveys. Differences in reference value ranges of EC (176-282 µS/cm) were as well not significant among seasonal surveys, but it was possible to evidence that this range of values is generally quite lower than those of groundwater from other areas of the Sibillini Mts. (e.g., western and central Sibillini Mts. 205-410 µS/cm - Cambi et al., 2022; Campiano catchment area 267-410 µS/cm - Mammoliti et al., 2022; Santa Scolastica Plain 459-661 µS/cm, high valley of Nera River 231-343 µS/cm - Martarelli et al., 2020; Sibillini Mts. Ridge 180-460 µS/cm - Boni et al., 1986).

The hydrochemical parameters are useful indicators, but they do not allow a definitive attribution of water origin or flow paths. Major ions and/or isotopic data, which are programmed for a further step of investigation, are needed to support a more definitive hydrochemical interpretation. In any case, the following considerations are here presented as first stage of discussion.

The EC values of groundwater may also depend on the interaction processes occurring along hydraulic pathways between waters and the rocks they come from, were hosted in or passed through. Thus, the small seasonal and annual differences among the hydrochemical parameter values in the study area may be compatible with a stable groundwater-hosting rocks interaction, likely associated with good persistence with time and space of the subsurface pathways within aquifers.

As concerns the EC of the various monitoring points within the high valley of the Tenna River (Table 4), in agreement with the conceptual model inferences shown in Figure 4, it is possible to consider that the Capotenna Spring waters have a quite low mean values of EC (about 220 µS/cm), suggesting they come from the Maiolica and subordinately from MUJ Aquifers. The relatively low EC values of the Capotenna Spring may reflect the distinctive geological and tectono-structural setting of the area. These values are consistent with a possible partial contribution of water from the perched Scaglia Aquifer, located in the Cima Cannafusto area to the west at higher elevations. During periods of intense rainfall, enhanced infiltration may facilitate downward percolation through the pervasively fractured Marne a Fucoidi deposits, allowing this water to reach the Capotenna Spring recharge area at lower topographic levels.

Contrarily, the Tenna River waters, at lower elevations, have mean EC values of 229-240 µS/cm and are compatible with a likely source mainly from the Basal Calcareous aquifers. These waters, despite they are from Basal Calcareous aquifer, are characterized by EC values not relatively high suggesting that their recharge area is likely not too far from their discharge area and the fast flow conditions does not permit a prolonged interaction with the anhydrites constituting the Triassic evaporites (ADB) at the base of the carbonate succession (e.g., Cambi et al., 2022; Mastrorillo et al., 2020; Mammoliti et al., 2022).

The Le Vene Creek waters (at right bank of the Tenna River) contrarily have lower mean EC values (about 209 µS/cm) despite locally seem to be fed by the Basal Calcareous Aquifer as the cited higher elevated sectors of the Tenna River. In any case, based on the integration of the conceptual model, structural setting, and field hydrochemical parameters, it is likely that at least part of its waters is from a perched hydrostructure featured by the Scaglia Aquifer located at higher levels in the surroundings of Sibilla Mt. peak.

At lower elevations, the Pisciarelle Springs waters (at right bank; mean EC about 246 µS/cm) exhibit slightly higher EC values than the Tenna River waters flowing at higher elevations. This difference likely suggests their origin from a distinct hydrostructure with respect to the Scaglia Aquifer, possibly fed by the Maiolica Aquifer that characterizes the hanging wall of the Sibillini Mts. Thrust (Table 4 and Fig. 4).

### *Some considerations on possible climatic and seismic near-field effects on groundwater*

The discharge data of high valley of the Tenna River available from previous pre-seismic studies (e.g., Regione Marche, 2022, and La Porta et al., 2018, in Figure 5; see also Baldoni, 2003) are not abundant, but they were anyway compared with those from present post-seismic study. Furthermore, the high variability of discharge values between low- (interval 0-0.05 $m^3$/s) and high-water seasons (0.45-0.95 $m^3$/s) did not allow to make clear comparison. Despite that, it was possible to evidence that two parameters had major importance for the comprehension of the discharge variations at the various sectors of the high valley of the Tenna River during 2017-2019 period. They are represented by climatic and seasonal variability of snow-rainfall and by post-seismic effects.

The groundwater resources of the Capotenna Spring suffered a slight progressive depletion related to recent years and particularly to spring 2017 (see March, April and May 2017 in Figure 3) dry recharge periods. Probably added to these climatic aspects (Fig. 5a), a possible near-field seismic contribution induced by the 2016-2017 severe seismic sequence may have enhanced this depletion, although its relative role cannot be quantified because of the limited availability of continuous pre-seismic monitoring data

It is likely evident, in any case, that substantial differences between pre- and post-seismic times did not occur along the Tenna stream at elevations lower than 990 m a.s.l. (Basal Calcareous Aquifer level; Fig. 5b). From the same figure it is also evident that the Tenna River discharge at these elevations decreased from 2018 to 2020 and reached a relative seasonal post seismic minimum value at the end of summer 2020 (this study) (Fig. 5b), not clearly connected to rainfall depletion (see Fig. 3).

## Conclusions

The Scaglia Aquifer likely contributes to the feeding by drainage of the groundwater supply works dug within the Maiolica Aquifer. In any case, during monitoring time, the Scaglia Aquifer at Capotenna had seldom sufficient hydraulic potential for allowing the drainage through the underlying local marly low permeability threshold.

The water emitted at Capotenna suddenly infiltered along the streambed at immediately lower elevations, in agreement with the role of recharge area played by this sector. The Maiolica and the subordinately relevant MUJ Aquifers, where the Capotenna spring has its origin, rarely had enough hydraulic potential to allow water overflow, excluding the tapped water.

Only at elevations lower than 1,100 m a.s.l., beyond the very low permeability threshold represented by the Marne di Monte Serrone, this aquifer has been able to release water. The further sector between 985-845 m a.s.l. evidenced complex hydraulic exchanges from groundwater to surface water and vice versa, likely due to the local tectonic fragmentation and the presence at relatively low depth of low permeable layers (Triassic evaporites; RSN, SCC, FUC marly formations) in this low elevated sector of the Basal Calcareous and Maiolica aquifers.

The hydrogeological scenario at the high valley of the Tenna River continuously evolved and the observed evolution is consistent with a partial recovery or a tendency towards pre-seismic conditions in the short-medium period. It is likely evident, in any case, that substantial differences between pre- and post-seismic periods did not occur along the Tenna stream at elevations lower than 990 m a.s.l. (Basal Calcareous Aquifer level).

Differences in reference value ranges of EC were not significant among seasonal surveys, but it was possible to evidence that this range of values is generally quite lower than those of groundwater from other areas of the Sibillini Mts. The relatively small seasonal and annual differences among the hydrochemical parameter values in the study area are consistent with a stable groundwater-hosting rocks interaction and good persistence with time and space of the subsurface pathways within aquifers.

The opportunity of maintaining yearly monitoring activities in areas affected by near-field coseismic effects is envisaged and it is suitable that they consist in at least two seasonal measurements at the selected control points, to have the opportunity to control the medium-long term variations of the evolving scenario.

Further investigations in the study area should include the definition of a more detailed conceptual model and the implementation of a numerical model, along with the implementation of chemical and isotopic analyses of waters, also in support to the recharge hypotheses now only based on electrical conductivity values.

The activities presented in this work contributed not only to a better comprehension of the hydrogeology of the study area, but they could also represent a contribution to the implementation of the literature about near-field coseismic effects on hydrogeological processes involving intramountainous areas. A possible near-field seismic inference induced by the 2016-2017 severe seismic sequence may have enhanced groundwater depletion due to recent snow and rainfall shortage, although its relative role cannot be quantified because of the limited availability of continuous pre-seismic monitoring data.

Finally, it is noteworthy to evidence a lesson learned from the increase of discharge as post-seismic effects, i.e. that the availability of new water resources is ephemeral, unless supported by long-term monitoring. In any case, this is a broader hydrogeological and management implication derived from both the present case study and the literature on the 2016-2017 Central Italy seismic sequence (e.g. Torbidone Spring in Santa Scolastica Plain and high valley of Nera River, Sibillini Mts.).

With respect to previous studies on the hydrogeological effects of the 2016-2017 seismic sequence in the Sibillini Mts., the main contribution of this paper is the reconstruction of a local conceptual model, the analysis of groundwater-surface water exchanges along the Tenna River, and the identification of elevation sectors with different hydraulic behavior.

### Acknowledgement

The Ente Parco Nazionale dei Monti Sibillini is warmly thanked for the support to survey activities. The anonymous referees are kindly acknowledged for their useful suggestions.

### Competing interest

The authors declare no competing interest.

### AI use declaration statement

The authors declare no AI was used for the preparation of any part of this paper.

### Author contributions

All authors contributed to data collection and processing, result interpretation, writing, reviewing and editing of the manuscript. All authors have read and agreed to the published version of the manuscript.

### Additional information

**DOI:** https://doi.org/10.7343/as-2026-946

**Reprint and permission information** are available writing to acquesotterranee@anipapozzi.it

**Publisher's note** Associazione Acque Sotterranee remains neutral with regard to jurisdictional claims in published maps and institutional affiliations.

## REFERENCES


Adinolfi Falcone, R., Carucci, V., Falgiani, A., Manetta, M., Parisse, B., Petitta, M., Rusi, S., Spizzico, M., & Tallini, M. (2012). Changes on groundwater flow and hydrochemistry of the Gran Sasso carbonate aquifer after 2009 L'Aquila earthquake. Italian Journal of Geosciences, 131(3), 459–474. https://doi.org/10.3301/IJG.2012.05

Annali Idrologici (1900-2012). Parte prima e parte seconda (sezioni di Roma, Pescara e Bologna) "*First part and second part (Sections of Rome, Pescara and Bologna*". Servizio Idrografico Ministero dei Lavori Pubblici/Servizio Idrografico e Mareografico Nazionale/Regioni Lazio, Abruzzo e Marche.

Baldoni, T. (2003). Idrogeologia dei Bacini dei Fiumi Ambro e Tennacola "*Hydrogeology of the Ambro and Tennacola River Basins*". Tesi di Laurea "Graduation thesis" a.a. 2002-2003. Corso di Laurea in Scienze Geologiche, Università degli Studi di Roma "La Sapienza".

Barberio, M.D., Barbieri, M., Billi, A., Doglioni, C., & Petitta, M. (2017). Hydrogeochemical changes before and during the 2016 Amatrice-Norcia seismic sequence (Central Italy). Scientific Reports, 7, 11735. https://doi.org/10.1038/s41598-017-11990-8

Berne, A., & Uijlenhoet, R. (2009). Elevation-dependent rainfall analysis in the Oria River basin. Hydrology and Earth System Sciences, 13(2), 229–239.

Boni, C., Baldoni, T., Banzato, F., Cascone, D., & Petitta, M. (2010). Hydrogeological study for identification, characterization and management of groundwater resources in the Sibillini Mountains National Park (central Italy). Italian Journal of Engineering Geology and Environment, 2, 21-39. https://doi.org/10.4408/ijege.2010-02.o-02

Boni, C., & Bono, P. (1982). Prima valutazione quantitativa dell'infiltrazione efficace sui sistemi carsici della piattaforma carbonatici laziale-abruzzese e nei sistemi di facies pelagica umbro-marchigiana-sabina (Italia centrale) "*First quantitative evaluation of the effective infiltration of the karst systems of the Latium-Abruzzi carbonate platform and of the Umbria-Marchean-Sabina pelagic facies systems (Central Italy)*". Geologia Applicata e Idrogeologia, 17, 427-436.

Boni, C., Bono, P., & Capelli, G. (1986). Schema idrogeologico dell'Italia Centrale "*Hydrogeological Sketch Map of Central Italy*". Memorie Società Geologica d'Italia, 35, 991-1012.

Boni, C., & Ruisi, M. (2002). Nuovi metodi di valutazione delle risorse idriche rinnovabili nel bacino dell'Aterno-Pescara "*New methods of evaluation of renewable water resources in the Aterno-Pescara river basin*". Proceedings of the 2019 World Water Day, Rome, February 12th, 1999.

Bredehoeft, J. (2005). The conceptualization model problem-surprise. Hydrogeology Journal, 13, 37-46.

Calamita, F., Coltorti, M., Deiana, G., Dramis, F., & Pambianchi, G. (1982). Neotectonic evolution and geomorphology of the Cascia and Norcia depressions. Geografia Fisica e Dinamica Quaternaria, 5, 263-276.

Calamita, F., & Deiana, G. (1988). The arcuate shape of the Umbria-Marche Apennines (Central Italy). Tectonophysics, 146, 139-147.

Cambi, C., Mirabella, F., Petitta, M., Banzato, F., Beddini, G., Cardellini, C., Fronzi, D., Mastrorillo, L., Tazioli, A., & Valigi, D. (2022). Reaction of the carbonate Sibillini Mountains Basal aquifer (Central Italy) to the extensional 2016–2017 seismic sequence. Scientific Reports, 12, 22428. https://doi.org/10.1038/s41598-022-26681-2

Centamore, E., Chiocchini, M., Deiana, G., Micarelli, A., & Pieruccini, U. (1971). Contributo alla conoscenza del Giurassico dell'Appenino umbro-marchigiano "*Contribution to the knowledge of the of the Jurassic of the Umbro-Marchean Apennine*". Studi Geologici Camerti, 1, 7–90.

Centamore, E., & Deiana, G. (Eds.) (1986). La geologia delle Marche "*The geology of the Marche*". Università di Camerino, Dipartimento di Scienze della Terra.

Chiaraluce, L., Di Stefano, R., Tinti, E., Scognamiglio, L., Michele, M., Casarotti, E., Cattaneo M., De Gori, P., Chiarabba, C., Monachesi, G., Lombardo, L., A., Valoroso, L., Latorre, D., & Marzorati, S. (2017). The 2016 central Italy seismic sequence: A first look at the mainshocks, aftershocks and source models. Seismological Research Letters, 88(3), 757–771. https://doi.org/10.1785/0220160221

Cipriani, A. (2016). Geology of the Mt. Cosce sector (Narni Ridge, Central Apennines, Italy). Journal of Maps, 12(1), 328–340. https://doi.org/10.1080/17445647.2016.1211896

Cipriani, A. (2019). Geological map of the central part of Narni-Amelia Ridge (Central Apennines, Italy). Geological Field Trips and Maps, 11(2.2), 1–26. https ://doi.org/10.3301/GFT.2019.04

Cipriani, A., Caratelli, M., & Santantonio, M. (2020a). Geological mapping reveals the role of Early Jurassic rift architecture in the dispersal of calciturbidites: New insights from the Central and Northern Apennines. Basin Research, 32, 1485–1509, https://doi org/10.1111/bre.12438

Cipriani, A., Zuccari, C., Innamorati, G., Marino, M. C., & Petti, F. M. (2020b). Mass-transport deposits from the Toarcian of the Umbria-Marche-Sabina Basin (Central Italy). Italian Journal of Geosciences, 139(1), 9–29. https://doi.org/10.3301/IJG.2019.14

Civico, R., Pucci, S., Villani, F., Pizzimenti, L., De Martini, P. M., Nappi, R., & Open EMERGEO Working Group (2018). Surface ruptures following the 30 October 2016 Mw 6.5 Norcia earthquake, central Italy. Journal of Maps, 14(2), 151–160. https://doi.org/10.1080/17445647.2018.1441756

Claesson, L., Skelton, A., Graham, C., Dietl, C., Mörth, M., Torssander, P., & Kockum, I. (2004). Hydrogeochemical changes before and after a major earthquake. Geology, 32, 641–644. https://doi.org/10.1130/G20542.1

Cox, S.C., Rutterb, H.K., Sims, A., Manga, M., Weir, J.J., Ezzy, T., White, P.A., Horton, T.W., & Scott, D. (2012). Hydrological effects of the MW 7.1 Darfield (Canterbury) earthquake, 4 September 2010, New Zealand. New Zealand Journal of Geology and Geophysics, 55(3), 231–247. https://doi.org/10.1080/00288306.2012.680474

Cugerone, K., Allamano, P., Salandin, A., & Barbero, S. (2012). Stima della precipitazione in siti di alta quota "*Evaluation of precipitation in high elevation sites*". Periodico AINEVA - Neve e Valanghe, 77, 36-43.

Curry, R.R., Emery, B.A., & Kidwell, T.G. (1994). Sources and magnitudes of increased streamflow in the Santa Cruz Mountains for the 1990 water year after the earthquake. In: Rojstaczer, S. (Ed.), The Loma Prieta, California, Earthquake of October 17, 1989-Hydrologic Disturbances. United States Geological Survey Professional Papers, 1551-E, 31–50.

Curzi, M., Cipriani, A., Aldega, L., Billi, A., Carminati, E., Van der Lelij, R., Vignaroli, G., & Viola, G. (2024). Architecture and permeability structure of the Sibillini Mts. Thrust and influence upon recent, extension-related seismicity in the central Apennines (Italy) through fault-valve behavior. Geological Society of America Bulletin, 136, 3-26. https://doi.org/10.1130/B36616.1

Deiana, G., & Pialli G. (1994). The structural provinces of the Umbro-Marchean Apennines. Memorie della Società Geologica Italiana, 48, 473-484.

Di Matteo, L., Dragoni, W., Azzaro, S., Pauselli, C., Porreca, M., Bellina, G., & Cardaci, W. (2020). Effects of earthquakes on the discharge of groundwater system: The case of the 2016 seismic sequence in the Central Apennines, Italy. Journal of Hydrology, 583, 124509. https://doi.org/10.1016/j.jhydrol.2019.124509

Enemark, T., Peeters, L. J., Mallants, D., & Batelaan, O. (2019). Hydrogeological conceptual model building and testing: A review. Journal of Hydrology, 569, 310-329. https://doi.org/10.1016/j.jhydrol.2018.12.007

Esposito, E., Pece, R., Porfido, S., & Tranfaglia, G. (2001). Hydrological anomalies connected to earthquakes in southern Apennines (Italy). Natural Hazards and Earth System Sciences, 1(3), 137–144. https://doi.org/10.5194/nhess-1-137-2001

Ferrario, M.F., & Livio, F. (2018). Characterizing the distributed faulting during the October 30, 2016, central Italy earthquake: A reference for fault displacement hazard assessment. Tectonics, 37(5), 1256-1273. https://doi.org/10.1029/2017TC004935

Fiddes, J., Endrizzi, S., & Gruber, S. (2020). Should altitudinal gradients of temperature and precipitation inputs be inferred from key parameters in snow-hydrological models? Hydrology and Earth System Sciences, 24(5), 2609–2625. https://doi.org/10.5194/hess-24-2609-2020

Fronzi, D., Banzato, F., Caliro, S., Cambi, C., Cardellini, C., Checcucci, R., Mastrotrillo, L., Mirabella, F., Petitta, M., Valigi, D., & Tazioli, A. (2020). Preliminary results on the response of some springs of the Sibillini Mountains area to the 2016-2017 seismic sequence. Italian Journal of Groundwater, 9(1), 19-25. https://doi.org/10.7343/as-2020-450

Fronzi, D., Mirabella, F., Cardellini, C., Caliro, S., Palpacelli, S., Cambi, C., Valigi, D., & Tazioli A. (2021). The role of faults in groundwater circulation before and after seismic events: Insights from tracers, water isotopes and geochemistry. Water, 13(11), 1499. https://doi.org/10.3390/w13111499

Galli, P., Peronace, E., Bramerini, F., Castenetto, S., Naso, G., Cassone, F., & Pallone F. (2016). The MCS intensity distribution of the devastating 24 August 2016 earthquake in central Italy (MW 6.2). Annals of Geophysics, 59. DOI: 10.4401/ag-7287

Gori, S., Falcucci, E., Galadini, F., Zimmaro, P., Pizzi, A., Kayen, R.E., Lingwall, B.N., Moro, M., Saroli, M., Fubelli, G., Di Domenica, A., & Stewart, J.P. (2018). Surface Faulting Caused by the 2016 Central Italy Seismic Sequence: Field Mapping and LiDAR/UAV Imaging. Earthquake Spectra, 34(4), 1585-1610. https://doi.org/10.1193/111417EQS236MR

Helfricht, K., Hartl, L., Koch, R., Marty, C., & Olefs, M. (2018). Obtaining sub-daily new snow density from automated measurements in high mountain regions. Hydrology and Earth System Sciences, 22, 2655–2668, 2018 https://doi.org/10.5194/hess-22-2655-2018

Kendall, M., Stuart, A., & Ord, J.K. (1983). The advanced theory of statistics. Volume 3. Charles Griffin and Company, London.

Kitagawa, Y., Koizumi, N., Takahashi, M., Matsumoto, N., & Sato, T. (2006). Changes in groundwater levels or pressures associated with the 2004 earthquake off the west coast of northern Sumatra (M9.0). Earth Planet Space, 58(2), 173–179

La Porta, G., Carosi, A., Cauzillo, C., Forconi, A., Pompei, L., Lorenzoni, M. (2018). Practical recommendation on the fittest approach to perform the captive breeding and restocking action on macrostigma trout. Part 3 - Habitat analysis. Deliverable A2-A3 Life+ TROTA Project (Action A.3). Dipartimento di Chimica, Biologia e Biotecnologie Università degli Studi di Perugia.

Lendvai, A., Ranzi, R., Peretti, G., Berbenni, F., Praolini, A., & Urbani, S. (2015) - Misura delle precipitazioni nevose mediante i pluviometri - stima degli errori sistematici e correzione delle serie storiche "*Snowfall measurement by rain gauges – systematic error evaluation and time series correction*". Periodico AINEVA - Neve e Valanghe, 84, 12-21.

Liu, C.Y., Chia, Y., Chung, P.Y., Lee, T.P., & Chiu, Y.C. (2023). Temporal Variation and Spatial Distribution of Groundwater Level Changes Induced by Large Earthquakes. Water, 15, 357. https://doi.org/10.3390/w15020357

Mammoliti, E., Fronzi, D., Cambi, C., Mirabella, F., Cardellini, C., Patacchiola, E., Tazioli, A., Caliro, S., & Valigi, D. (2022). A holistic approach to study groundwater-surface water modifications induced by strong earthquakes: The case of Campiano catchment (Central Italy). Hydrology, 9(6), 97. https://doi.org/10.1193/111417EQS236MR

Martarelli, L., Gafà, R.M., La Vigna, F., Monti, G.M., Puzzilli, L.M., Ruscito, V., & Silvi, A. (2020). Studio delle variazioni delle condizioni di pericolosità da frana e da fenomeni di dissesto lungo la rete sentieristica e della circolazione delle acque sotterranee e superficiali avvenute in seguito agli eventi sismici del 2016 e 2017. Relazione finale delle attività idrogeologiche svolte "*Study on the variations of landslide hazard along the paths and of the groundwater and surface water conditions induced by seismic sequence 2016-2017. Final report on hydrogeological activities*". ISPRA–Ente Parco Nazionale dei Monti Sibillini. Servizio Geologico d'Italia - ISPRA, Roma. Unpublished report with hydrogeological maps, July 2020.

Mastrorillo, L., Baldoni, T., Banzato, F., Boscherini, A., Cascone, D., Checcucci, R., Petitta, M., & Boni, C. (2009). Analisi idrogeologica quantitativa del dominio carbonatico umbro "*Quantitative hydrogeological analysis of the carbonate domain of the Umbria Region*". Italian Journal of Engineering Geology and Environment, 1(2009), 137-155.

Mastrorillo, L., Saroli, M., Viaroli, S., Banzato, F., Valigi, D., & Petitta, M. (2020). Sustained post-seismic effects on groundwater flow in fractured carbonate aquifers in Central Italy. Hydrological Processes, 34, 1167–1181.

Mastrorillo, L., Viaroli, S., & Petitta, M. (2023). Co-Occurrence of Earthquake and Climatic Events on Groundwater Budget Alteration in a Fractured Carbonate Aquifer (Sibillini Mts. - Central Italy). Water, 15(13), 2355. https://doi.org/10.3390/w15132355

Mohr, C.H., Manga, M., Wang, C.Y., & Korup, O. (2016). Regional changes in streamflow after a megathrust earthquake. Earth and Planetary Science Letters. https://doi.org/10.1016/j.epsl.2016.11.013

Nanni, T., Vivalda, P.M., Palpacelli, S., Marcellini, M., & Tazioli, A. (2020). Groundwater circulation and earthquake-related changes in hydrogeological karst environments: a case study of the Sibillini Mountains (central Italy) involving artificial tracers. Hydrogeology Journal, 28, 2409–2428. https://doi.org/10.1007/s10040-020-02207-w

Petitta, M., Mastrorillo, L., Preziosi, E., Banzato, F., Barberio, M.D., Billi, A., Cambi, C., De Luca, G., Di Carlo, G., Di Curzio, D., Di Salvo, C., Nanni, T., Palpacelli, S., Rusi, S., Saroli, M., Tallini, M., Tazioli, A., Valigi, D., Vivalda, P., & Doglioni. C. (2018). Water-table and discharge changes associated with the 2016–2017 seismic sequence in central Italy: hydrogeological data and a conceptual model for fractured carbonate aquifers. Hydrogeology Journal, 26, 1009-1026. https://doi.org/10.1007/s10040-017-1717-7

Petitta, M., Primavera, P., Tuccimei, P., & Aravena, R. (2011). Interaction between deep and shallow groundwater systems in areas affected by quaternary tectonics (central Italy): a geochemical and isotope approach. Environmental Earth Science, 63, 11–30.

Pierantoni, P., Deiana, G., & Galdenzi, S. (2013). Stratigraphic and structural features of the Sibillini mountains (Umbria-Marche Apennines, Italy). Italian Journal of Geosciences ,132(3), 497-520.

Regione Lazio (2022). Agenzia Regionale Protezione Civile - Servizio Idrografico – Rete idrometeorologica "*Regional Civil Protection Agency – Hydrographical Service – Hydrometeorological network*". https://temporeale.regione.lazio.it/aegis/map/map2d - last access May 2023.

Regione Marche (2022). Centro Funzionale Multirischi della Protezione Civile - Sistema Informativo Regionale Meteo-Idro-Pluviometrico "*Civil Protection Multirisk Functional Centre - Meteo-Hydro-Pluviometric Regional Information System*". https://www.regione.marche.it/Regione-Utile/Protezione-Civile/Progetti-e-Pubblicazioni/Meteo - last access May 2023.

Regione Umbria (2022). Servizio Idrografico – Stazioni Meteo – Dataset - Open Data Umbria "*Umbria Region – Hydrographical Service – Meteo Stations – Dataset - Open Data Umbria*". https://dati.regione.umbria.it/dataset/sir_stazioni_meteo - last access May 2023.

Roquier, B., Fluixa Sanmartin, J., Brauchli, T., Baracchini, T., Garcia Hernandez, J., Foehn, A., Paredes Arquiola, J., & De Cesare, G. (2022). RS MINERVE Software Manuals – Technical documentation: Hydrological models. Retrieved from CREALP (Centre de Recherche sur l'Environnement Alpin) website https://crealp.github.io/rsminerve-releases/tech_hydrological_models.html - last access May 2023.

Rosen, M. R., Binda, G., Archer, C., Pozzi, A., Michetti, A. M., & Noble, P. J. (2018). Mechanisms of earthquake-induced chemical and fluid transport to carbonate groundwater springs after earthquakes. Water Resources Research, 54, 5225–5244. https://doi.org/10.1029/2017WR022097

Rossi, A., Tertulliani, A., Azzaro, R., Graziani, L., Rovida, A., Maramai, A., Pessina, V., Hailemikael, S., Buffarini, G., Bernardini, F., Camassi, R., Del Mese, S., Ercolani, E., Fodarella, A., Locati, M., Martini, G., Paciello, A., Paolini, S., Arcoraci, L., Castellano, C., Verrubbi, V., & Stucchi, M. (2019). The 2016-2017 earthquake sequence in central Italy: macroseismic survey and damage scenario through the EMS-98 intensity assessment. Bulletin of Earthquake Engineering, 17, 2407-2431. https://doi.org/10.1007/s10518-019-00556-w

Santantonio, M., Cipriani, A., Fabbi, S., & Meister, C. (2022). Constraining the slip rate of Jurassic rift faults through the drowning history of a carbonate platform. Terra Nova, 34(2), 137-145.

Santantonio, M., Innamorati, G., Cipriani, A., Antonelli, M., & Fabbi, S. (2024). An exceptionally well-preserved Jurassic plateau-top to marginal escarpment in the Northern Apennines (Central Italy): sedimentological, palaeontological and palaeostructural features. Journal of Iberian Geology, 50(2), 253-268.

Smeraglia, L., Billi, A., Carminati, E., Cavallo, A., & Doglioni, C. (2017). Field- to nano-scale evidence for weakening mechanisms along the fault of the 2016 Amatrice and Norcia earthquakes, Italy. Tectonophysics, 712–713, 156–169. https://doi.org/10.1016/j.tecto.2017.05.014

Sneyers, R. (1990). On the statistical analysis of series of observations. Technical Note, N.143, World Meteorological Organization, Geneva, Switzerland.

Testa, A., Boncio, P., Di Donato, M., Mataloni, G., Brozzetti, F., & Cirillo, D. (2019). Mapping the geology of the 2016 Central Italy earthquake fault (Mt. Vettore–Mt. Bove fault, Sibillini Mts.): geological details on the Cupi-Ussita and Mt. Bove-Mt. Porche segments and overall pattern of coseismic surface faulting. Geological Field Trips and Maps, 11.

Turc, L. (1961). Estimation of irrigation water requirements, potential evapotranspiration: a simple climate formula evolved up to date. Annual of Agronomy, 12, 13-49.

Valigi, D., Cardellini, C., Mirabella, F., Nanni, T., Tazioli, A., Petitta, M., & Caliro, S. (coords.) (2020a). Caratterizzazione dei sistemi idrogeologici del territorio umbro influenzato dagli eventi sismici del 26-30 ottobre 2016 e valutazione degli effetti del sisma sull'approvvigionamento idrico. Rapporto finale "*Characterization of the hydrogeological systems of the Umbria territory influenced by the seismic events of October 26-30th 2016 and evaluation of the seismic effects on the water supply. Final report*". Perugia, Regione Umbria. Unpublished report, July 2020.

Valigi, D., Fronzi, D., Cambi, C., Beddini, G., Cardellini, C., Checcucci, R., Mastrorillo, L., Mirabella, F., & Tazioli, A. (2020b). Earthquake-induced spring discharge modifications: the Pescara di Arquata Spring reaction to the August-October 2016 central Italy Earthquakes. Water (Switzerland), 12 (3), 1-18. https://dx.doi.org/10.3390/w12030767

Valigi, D., Mastrorillo, L., Cardellini, C., Checcucci, R., Di Matteo, L., Frondini, F., Mirabella, F., Viaroli, S., & Vispi, I. (2019). Springs discharge variations induced by strong earthquakes: the Mw 6.5 Norcia event (Italy, October 30th, 2016). Rendiconti Online della Società Geologica Italiana, 47, 141–146.

Viaroli, S., Mirabella, F., Mastrorillo, L., Angelini, S., & Valigi, D. (2021). Fractured carbonate aquifers of Sibillini Mts. (Central Italy). Journal of Maps, 17(2), 140-149. https://doi.org/10.1080/17445647.2021.1894252

Villani, F., Civico, R., Pucci, S., Pizzimenti, L., Nappi, R., De Martini, P.M., & Open EMERGEO Working Group (2018). A database of the coseismic effects following the 30 October 2016 Norcia earthquake in central Italy. Scientific Data, 5, 180,049. https://doi.org/10.1038/sdata.2018.49

Wang, C.Y., & Manga, M. (2010). Hydrologic responses to earthquakes and a general metric. Geofluids, 10(1–2), 206–216. https://doi.org/10.1111/j.1468-8123.2009.00270.x

Weaver, K.C., Cox, S.C., Townend, J., Rutter, H., Hamling, I.J., & Holden, C. (2019). Seismological and Hydrogeological Controls on New Zealand-Wide Groundwater Level Changes Induced by the 2016 Mw 7.8 Kaikoura Earthquake. Geofluids, 2019, 9809458.

Yan, R., With, H., & Wang, R. (2014). Groundwater level changes induced by the 2011 Tohoku earthquake in China mainland. Geophysical Journal International, 199(1), 533–548. https://doi.org/10.1093/gji/ggu196